CENS Lunch Seminar

- ^{17}C spectroscopy using the SAMURAI spectrometer:
  π + ρ tensor force effect on the *p-sd* cross shell interaction

- **New experiment idea using the SAMURAI spectrometer:**
  π + ρ tensor force effect on the Z = 6 shell gap

- **Research idea for KoBRA:**
  Isosclar strength of the low-energy dipole excitation
  (suggested by Dr. P. Papakonstantinou)

Sunji KIM

NN interaction

- The oldest theory of nuclear forces was presented by Hideki Yukawa. In 1935, Yukawa postulated the existence of a massive particle (meson) in ~200 MeV to be responsible for NN interaction.

Hideki Yukawa
Nobel Prize in 1949

- In 1940, Hans A. Bethe demonstrated that the tensor force is formulated with the coupling due to pion with explicit reference to the tensor force and its effect on the deuteron property.

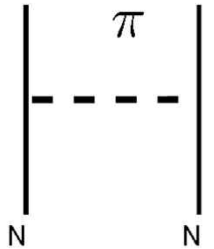

- Besides the π-meson exchange, the ρ-meson contributes to the tensor force for the short range part.

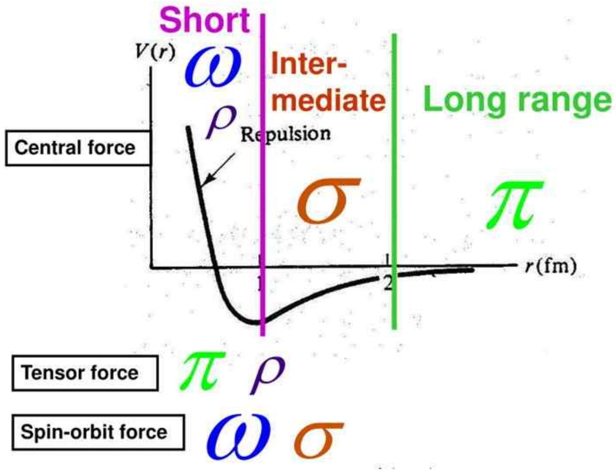

Tensor force effect

NN interaction: Tensor force

- Tensor force
  - A non-central force depending on the relative spins of two nucleons, $V(\vec{r})$
- The simplest nucleus, Deuteron
  - The observed magnetic moment and non-zero electric quadrupole moment value for the deuteron points to their being some orbital motion present (L>0).
  - It turns out that the ground state wave function must be a mixture of two angular momentum states, L = 0 and 2 (in 4%).
  - Wave functions with mixed L values suggested the presence of a non-central tensor component in the NN interaction.

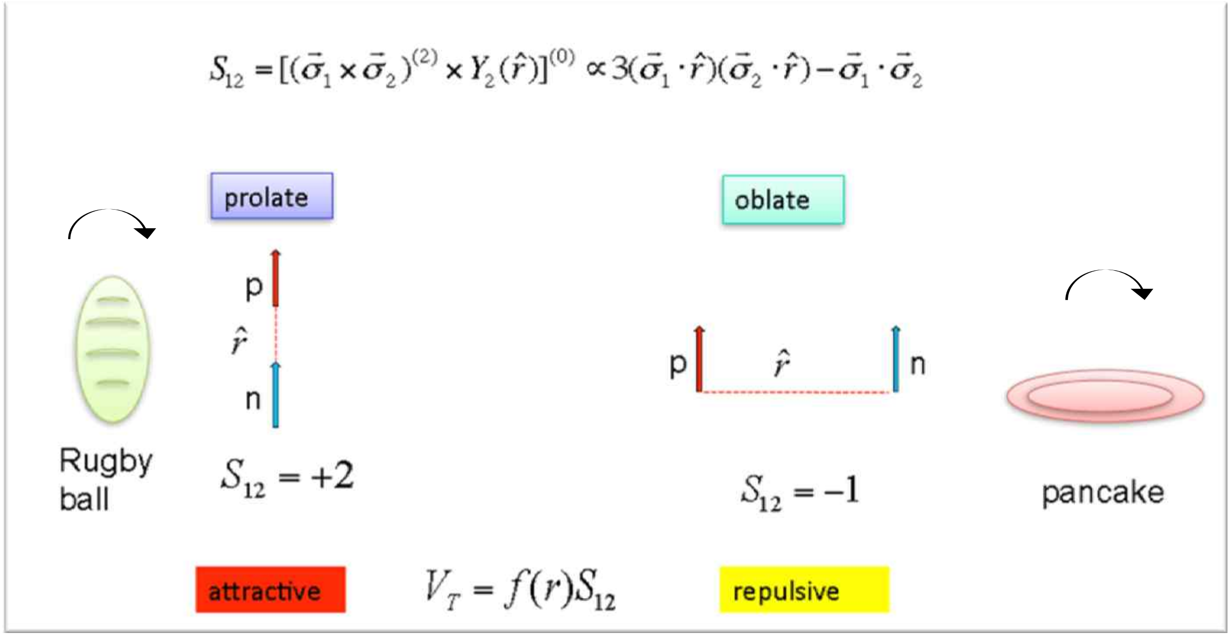

Schematic picture of the expectation values of the tensor operator S_{12}

(H. Sagawa and G. Colo, PPNP 76, 76 (2014))

Tensor force

- Tensor force effect and orbital motion
  ($j_{>}$=ℓ+1/2, $j_{<}$=ℓ-1/2)

- Tensor force acting two nucleons on orbits j, j'

Narrow wave function by the large relative momentum

Stretched wave function by the small relative momentum

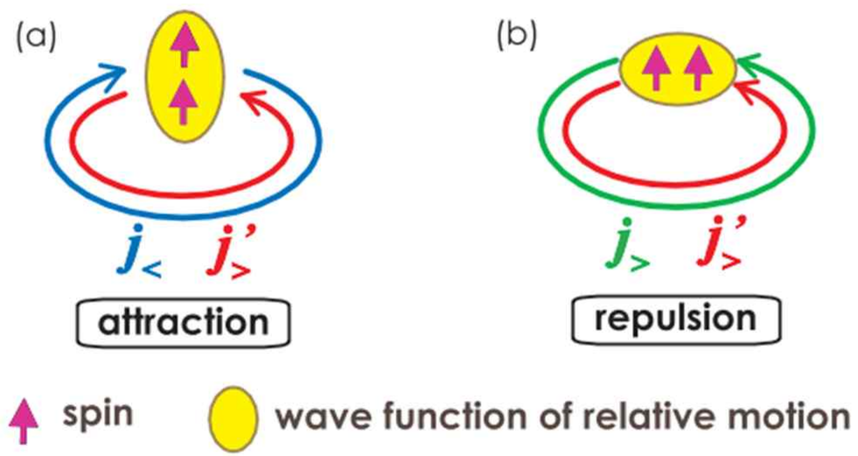

- Monopole interaction of the tensor force

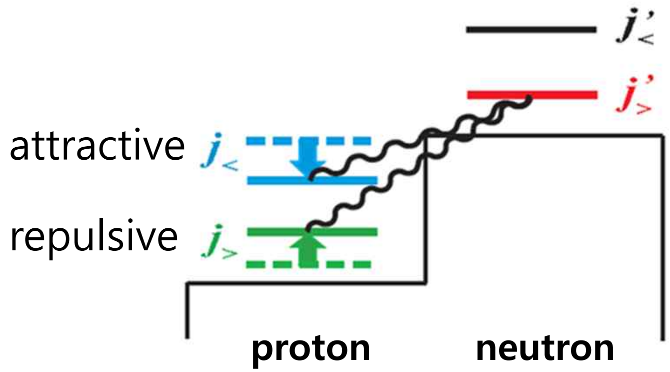

(T.Otsuka et al., PRL 95, 232502 (2005))

Tensor force contribution in *p-sd* cross-shell interaction

- When the tensor interaction arising from π+ρ meson-exchange is considered in *psd* region, **the π+ρ tensor force in *p-sd* cross-shell interaction is stronger** than that in WBT and WBP in the T=0 channel, more attractive $<p_{1/2}d_{5/2}|V|p_{1/2}d_{5/2}>$ and more repulsive in $<p_{3/2}d_{5/2}|V|p_{3/2}d_{5/2}>$.

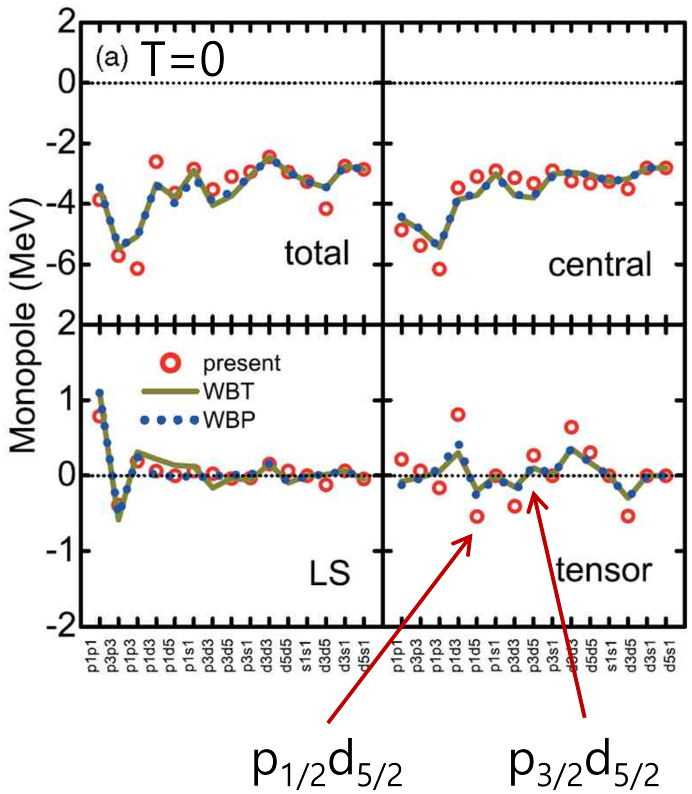

(C.Yuan et al., PRC 85, 064324 (2012))

Tensor force contribution in *p-sd* cross-shell interaction

- In neutron-rich C isotopes, repulsive force in $\langle p_{3/2}d_{5/2}|V|p_{3/2}d_{5/2}\rangle$ becomes active; the stronger repulsion in the π+ρ tensor force pushes up the neutron $d_{5/2}$ orbit more, resulting in larger shell gap between *p-sd* orbits in neutrons than oxygen isotopes. Therefore, the E_x of the cross-shell states such as $1/2^-_1$ and $3/2^-_1$ increase.

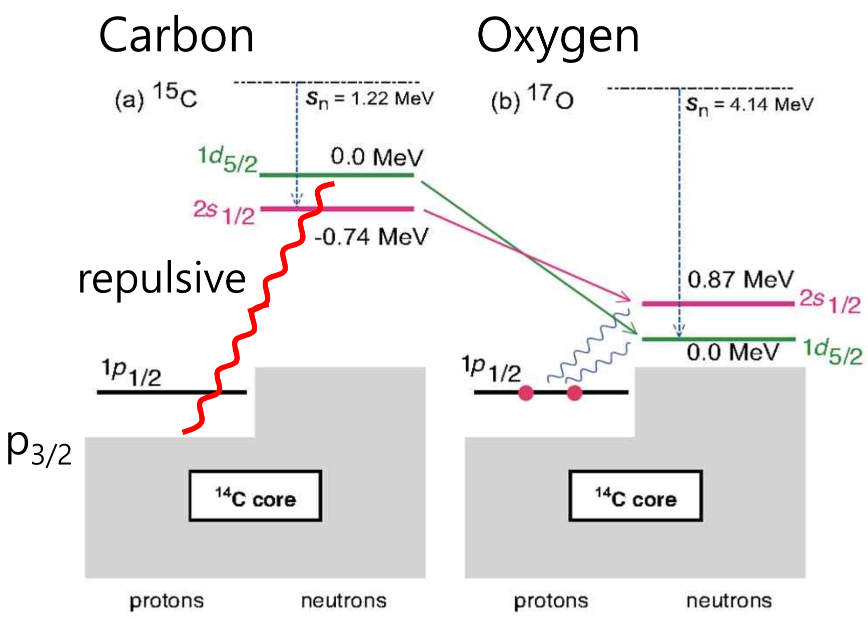

(T.Otsuka et al., arXiv:1805.06501 [nucl-th])

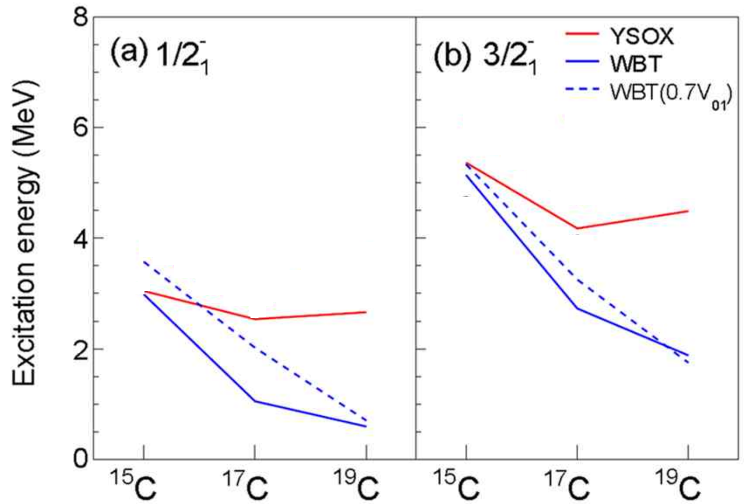

YSOX: an interaction employing V_{MU} including **the π+ρ tensor force for *p-sd* cross-shell interaction**
(C.Yuan et al., PRC 85, 064324 (2012))

WBT($0.7V_{01}$): a modified WBT having 30% reduced diagonal matrix elements of two-body effective interaction in I=0 and T=1 for *sd* neutrons
(H.Ueno et al., PRC 87, 034316 (2013))

Experiment

- Invariant mass spectroscopy of ^{17}C in $\mathbf{^{12}C(^{18}C,^{17}C^{*}\rightarrow ^{16}C+n)}$ at 245 MeV/nucleon using the SAMURAI spectrometer at RIKEN

The SAMURAI spectrometer was designed for kinematically complete experiments such as the invariant-mass spectroscopy of particle-unbound states in exotic nuclei, by detecting heavy fragments and projectile-rapidity nucleons in coincidence.

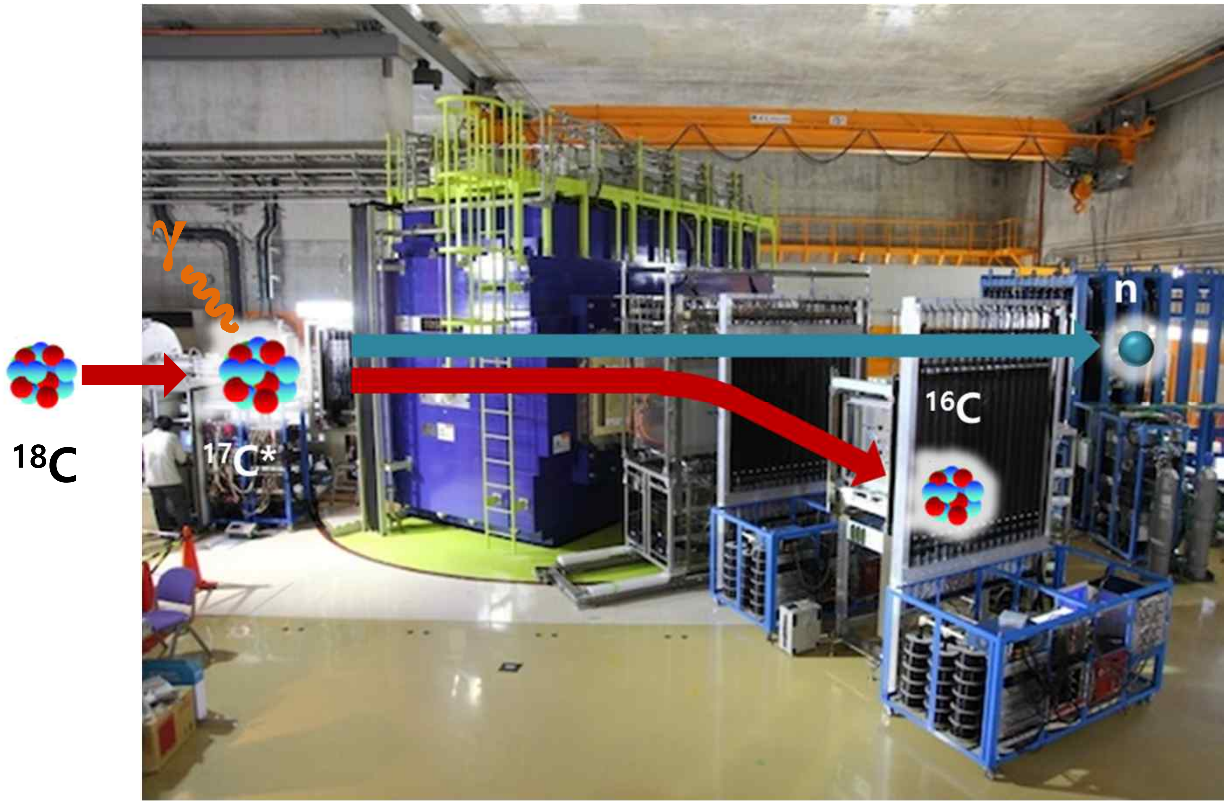

Invariant mass method

- Invariant mass

$$E_{inv} = \sqrt{(E_n + E_f)^2 - \left|\boldsymbol{P}_n + \boldsymbol{P}_f\right|^2}$$

- Relative energy

$$E_{rel} = E_{inv} - (M_n + M_f)$$

- Excitation energy

$$E_x = E_{rel} + S_n(+E_\gamma)$$

f:^{16}C fragment n: neutron

Experiment

- Relative energy spectrum of $^{17}C^*$

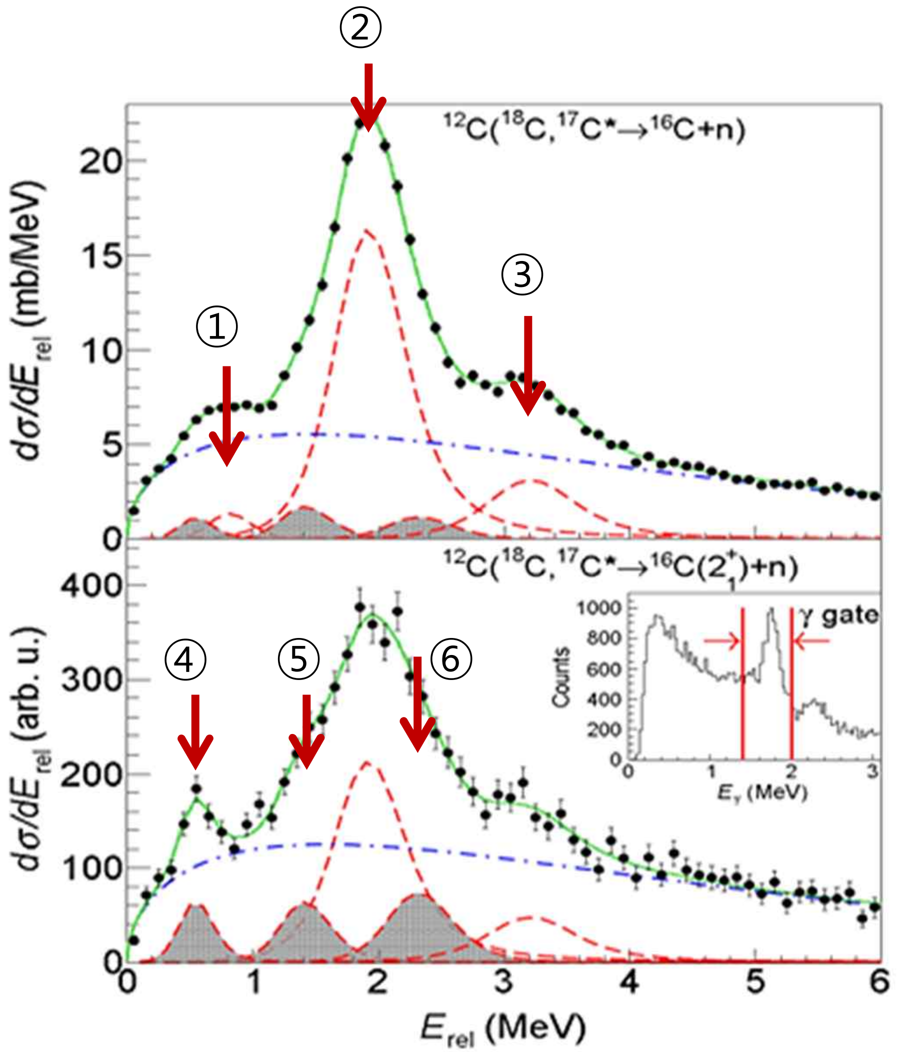

E_{rel} (MeV)	E_x (MeV)	J^π
① 0.81(5)	1.55(5)	$(5/2_2^+)$
② 1.92(1)	2.66(2)	$1/2_1^-$
③ 3.22(2)	3.96(3)	$3/2_1^-$
④ 0.54(6)	3.04(6)	$(3/2_2^+)$
⑤ 1.41(4)	(3.9($\rightarrow ^{16}C(2_1^+)$), 6.1($\rightarrow ^{16}C(2_2^+)$))	$(3/2_1^-, 3/2_3^-)$
⑥ 2.30(3)	(4.8($\rightarrow ^{16}C(2_1^+)$), 6.1($\rightarrow ^{16}C(0_2^+)$))	$(1/2_2^+, 3/2_2^-, 1/2_2^-)$

Experiment

- J^{π} assignment for resonance ①, ②, and ③

- Momentum distributions of ② and ③

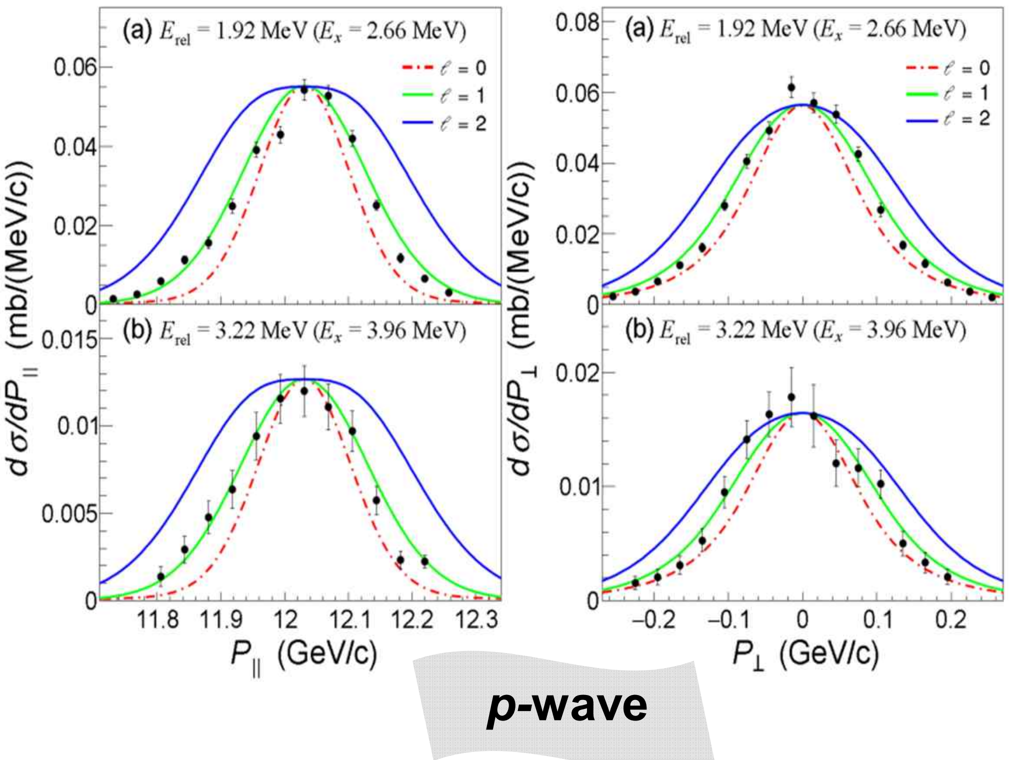

Using the reaction theory based on eikonal method, the orbital angular momentum can be determined.

Calculation by MOMDIS
(C. A. Bertulani and A. Gade, CPC 175, 372 (2006))

- Energy level diagram of ^{17}C in YSOX

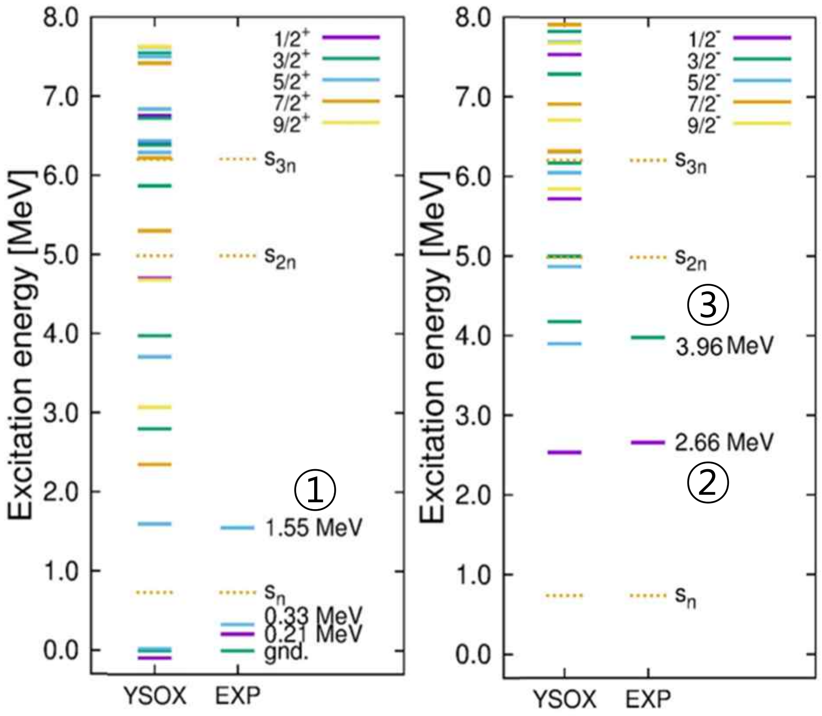

Calculation by NuShellX in YSOX in psd

Experiment

- J^{π} assignment for resonance ④, ⑤, and ⑥

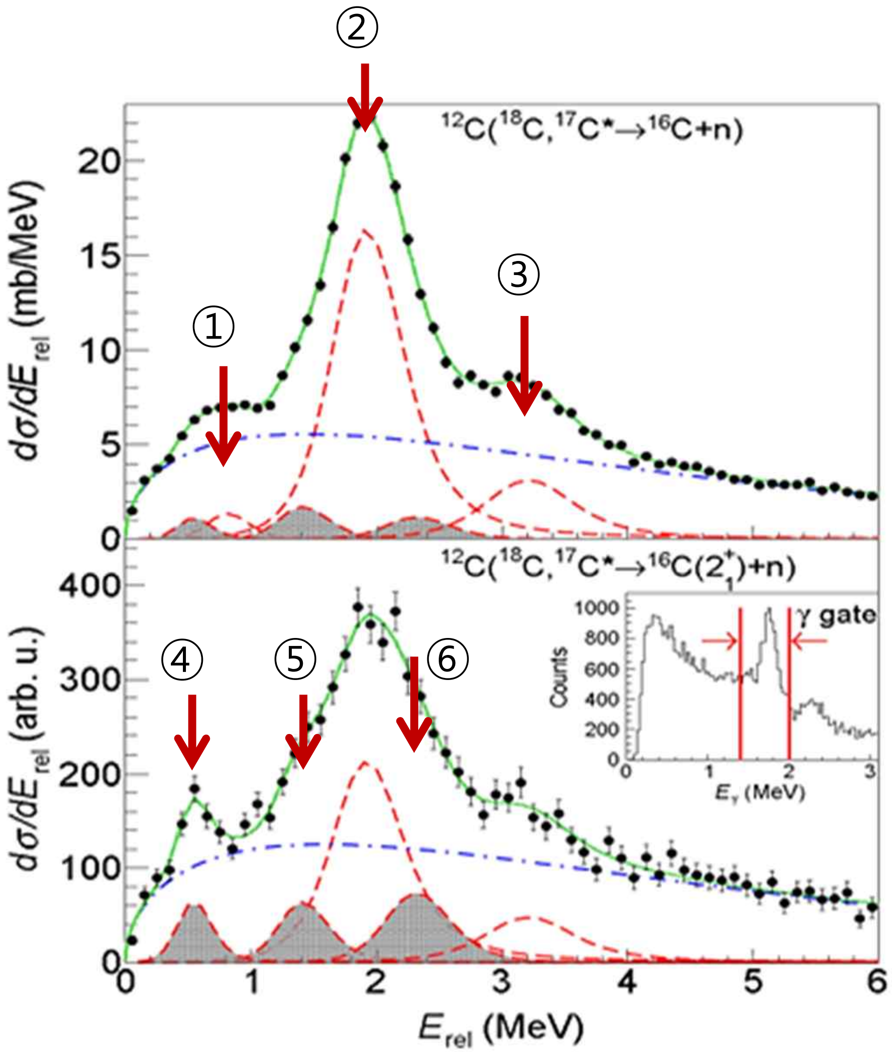

J^{π} candidates by 1n knockout from ^{18}C

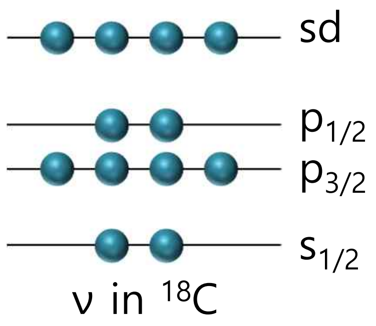

$1/2^-_{1,2}$, $3/2^-_{1,2,3}$,
$1/2^+_2$, $3/2^+_{2,3}$, $5/2^+_{2,3}$

Branching ratios and E$_{\text{decay}}$ of the candidate states, decaying into ^{16}C(2^+_1) or higher-lying ^{16}C states having final ^{16}C(2^+_1) level, were calculated to identify J^{π} of the resonance ④, ⑤, and ⑥.

Single-particle width: $\Gamma_{s.p.}$
with Woods-Saxon potential
obtained by main-aoi-70p0_double code

Partial width: $\Gamma_i = C^2S \cdot \Gamma_{s.p.}$

Branching ratio: $\mathrm{B.R.}^{\mathrm{th}} = \Gamma_i / \sum_i \Gamma_i$

Experiment

- J^{π} assignment for resonance ④, ⑤, and ⑥

Branching ratios and E_{decay} of candidate states

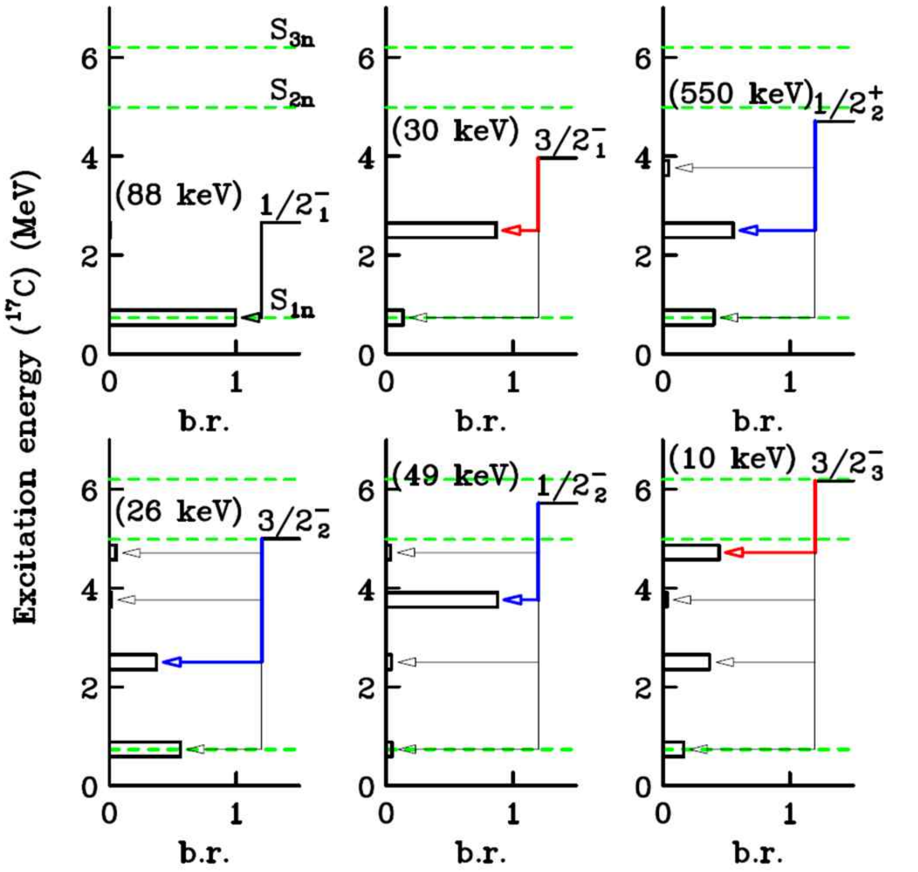

E_{rel} (MeV)	E_x (MeV)	J^{π}
① 0.81(5)	1.55(5)	NEW $(5/2^+_2)$
② 1.92(1)	2.66(2)	$1/2^-_1$
③ 3.22(2)	3.96(3)	$3/2^-_1$
④ 0.54(6)	3.04(6)	$(3/2^+_2)$
⑤ 1.41(4) (→)	(3.9(→^{16}C(2^+_1)), 6.1(→^{16}C(2^+_2)))	$(3/2^-_1$, $3/2^-_3)$ NEW possible branch
⑥ 2.30(3) (→)	(4.8(→^{16}C(2^+_1)), 6.1(→^{16}C(0^+_2)))	$(1/2^+_2$, $3/2^-_2$, $1/2^-_2)$

Cross-shell states in ^{17,19}C

- In neutron-rich C isotopes, due to **the π+ρ tensor force the stronger repulsion** between the $p_{3/2}$ protons and $d_{5/2}$ neutrons pushes up the neutron $d_{5/2}$ orbit more, resulting in large shell gap between *p-sd* orbits and increasing the E_x of the cross-shell states such as $1/2^-_1$ and $3/2^-_1$.

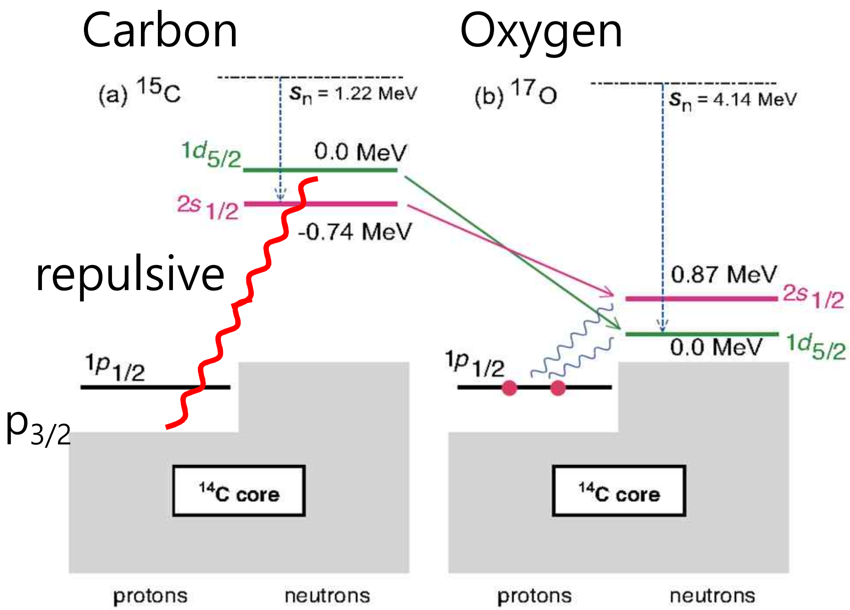

(T.Otsuka et al., arXiv:1805.06501 [nucl-th])

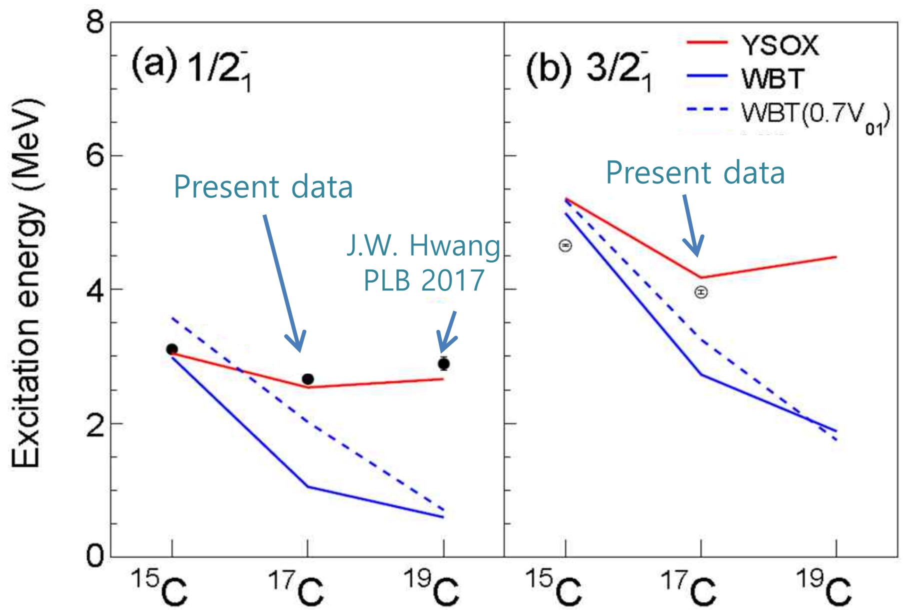

New experiment idea
using the SAMURAI spectrometer

Change of the Z = 6 shell gap in neutron-rich carbon isotopes

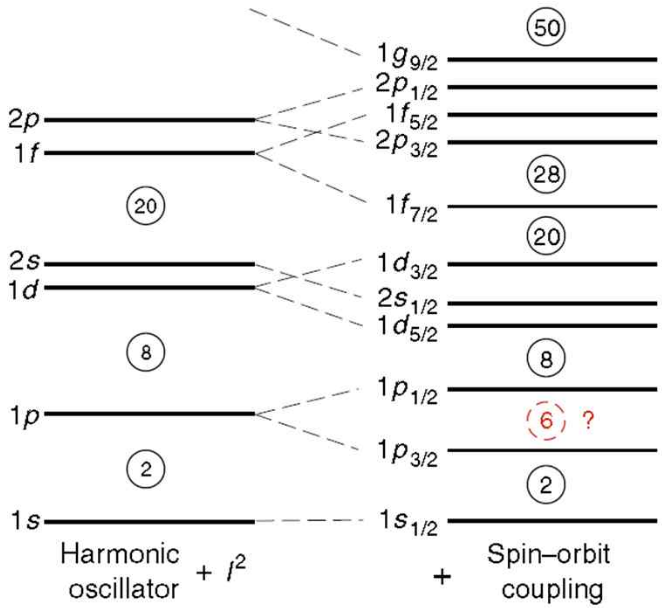

'Evidence for prevalent Z = 6 magic number in neutron-rich carbon isotopes'
(D. T. Tran et al., Nature Commun. 9, 1594 (2018))

Proposed Experiment

- **Proposed Experiment**

Change of the Z = 6 shell gap in neutron-rich carbon isotopes

: Missing mass spectroscopy of $^{15,17,19}C$ by the quasifree one-proton knockout reaction

- **Experiment purpose**

Investigation of the proton shell evolution at Z = 6 in neutron-rich C isotopes and verification of the effect of the π+ρ tensor force

Physics Motivation

- **Change of the Z = 6 shell gap in neutron-rich carbon isotopes**

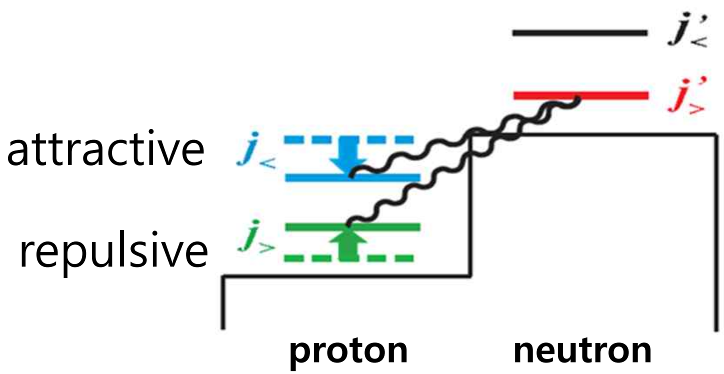

Monopole interaction of the tensor force
($j_>=\ell+1/2$, $j_<=\ell-1/2$)
(T.Otsuka et al., PRL 95, 232502 (2005))

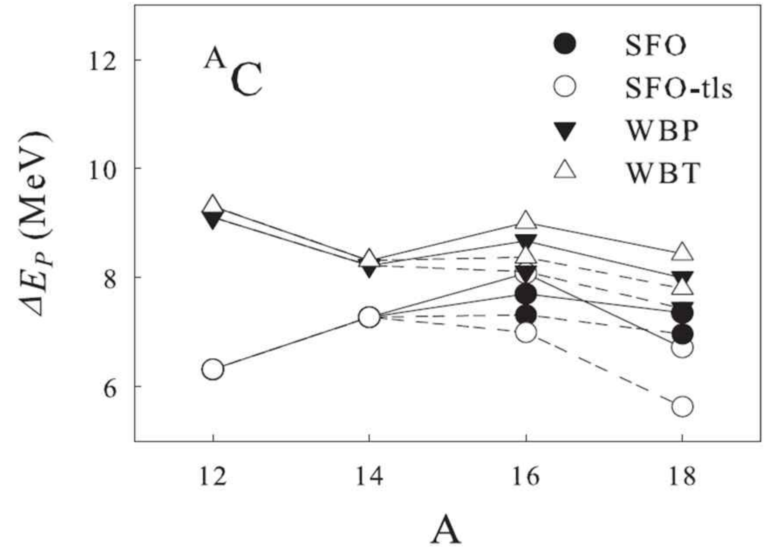

(T. Suzuki and T. Otsuka, PRC 78, 061301 (2008))

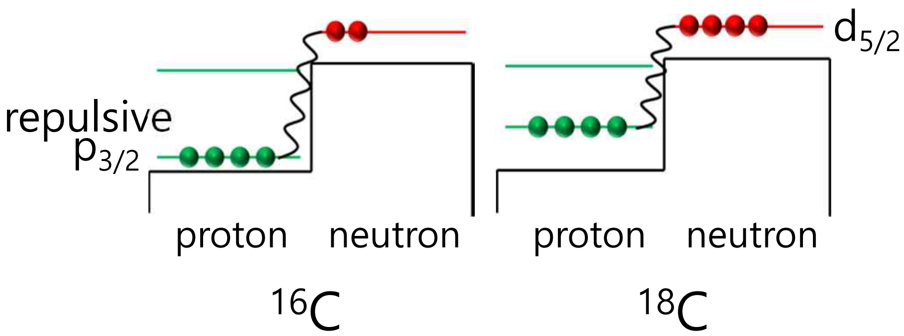

The ΔE_p is predicted to decrease by adding neutrons in $d_{5/2}$ orbit. The amount of the reduction is conspicuous for SFO-tls, including **the tensor interaction arising from π + ρ meson-exchange for *p-sd* cross-shell interaction.**

➡ Identification of the Z = 6 shell gap dependence on the shell models and Verification of the π + ρ tensor force contribution for *p-sd* cross-shell interaction.

Experimental Method

Neutron decay channel

Invariant mass spectroscopy

$$E_{inv} = \sqrt{(E_n + E_f)^2 - \left|\boldsymbol{P}_n + \boldsymbol{P}_f\right|^2}$$

- (p(^{16,18,20}N,^{15,17,19}C))

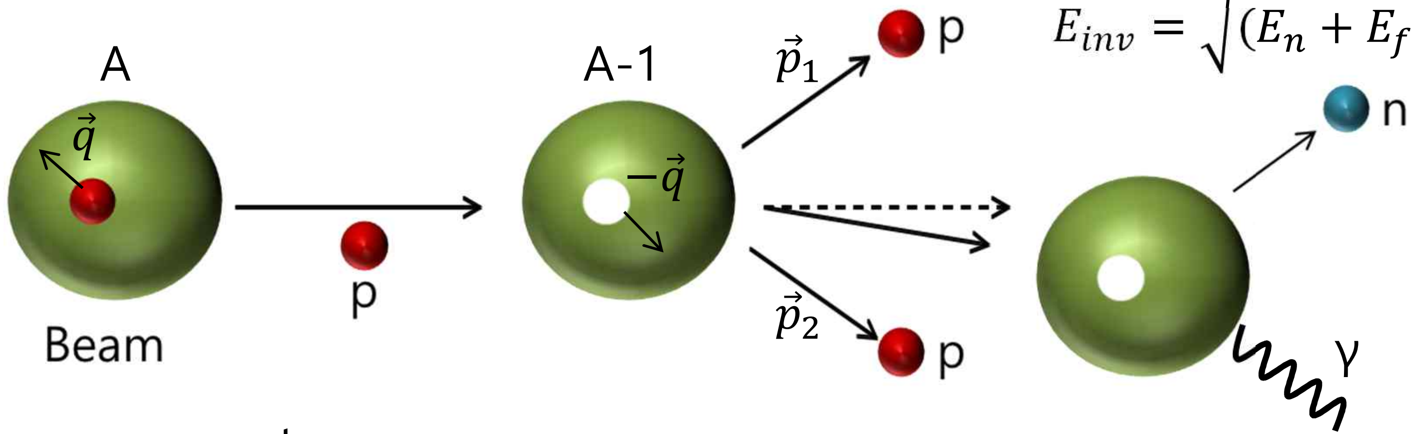

γ-ray spectroscopy

Missing mass spectroscopy

$$S_p = \left(2M_p + M_{A-1}\right) - \left(M_p + M_T\right)$$

$$= (1-\gamma)M_p - \gamma(T_1 + T_2) + \beta\gamma\left(p_{1||} + p_{2||}\right) - \frac{q^2}{2M_{A-1}}$$

(S. Kawase et al., PTEP 021D01 (2018))

Excitation energy

Identification of the knocked-out proton orbits and energy difference

Experimental Setup

- **PFAD and CATANA+ system for the missing mass and γ-ray spectroscopy**

: a prototype system of CATANA+ and STRASSE
(Silicon Tracker for Radioactive-nuclei Studied at SAMURAI Experiments)

From the simulation of $^{11}Li(p,2p)^{10}He$ at 200 MeV/u with a 0.1-mm CH_2 target,
two proton coincidence efficiency = ~7% and
energy resolution = 0.7 MeV at 10 MeV in σ
(Y. Sun, private communication)

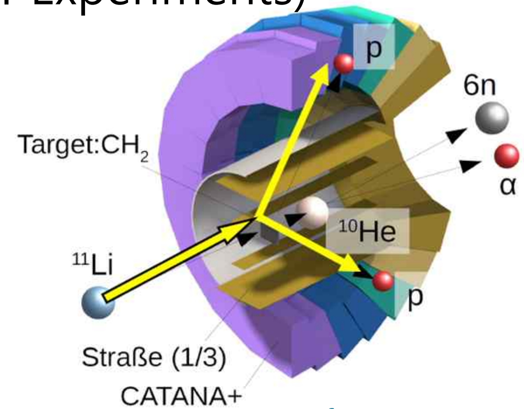

(Courtesy of Y. Sun)

- **Standard SAMURAI setup for the invariant mass spectroscopy**

: SBT1, SBT2, BDC1, BDC2, SAMURAI magnet, FDC1, FDC2, HODF, and NEBULA PLUS

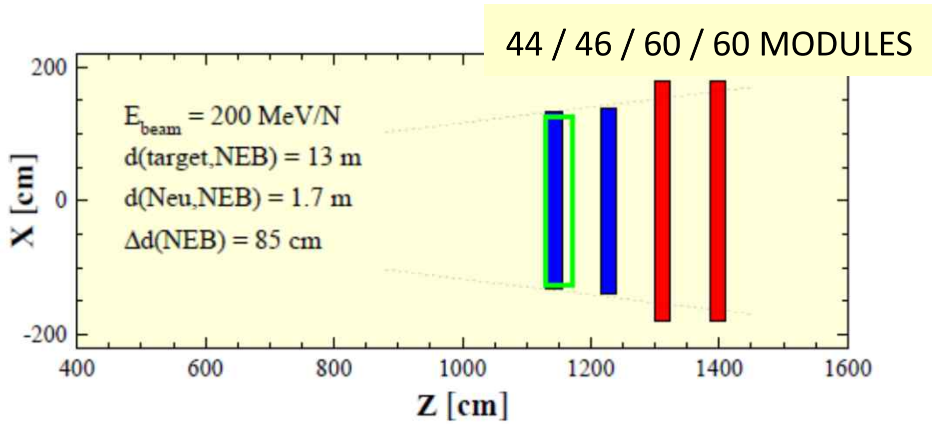

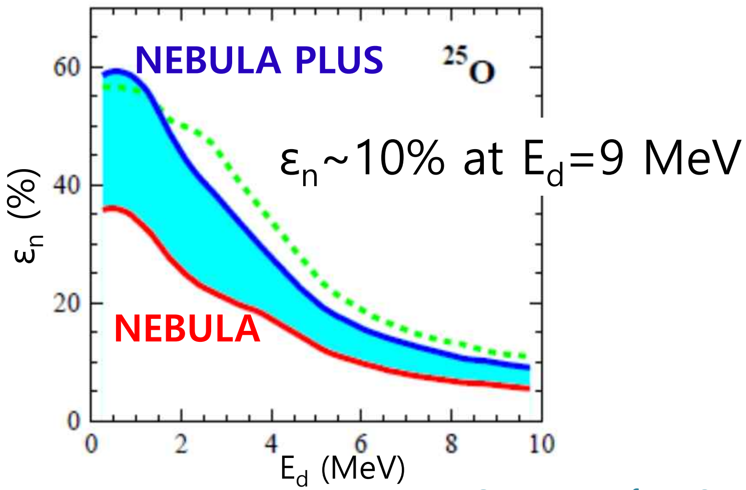

(Courtesy of N. Orr)

Predicted Results: Excitation energies and Cross sections

- **Expected cross sections of the states predicted in (p,2p) reaction**

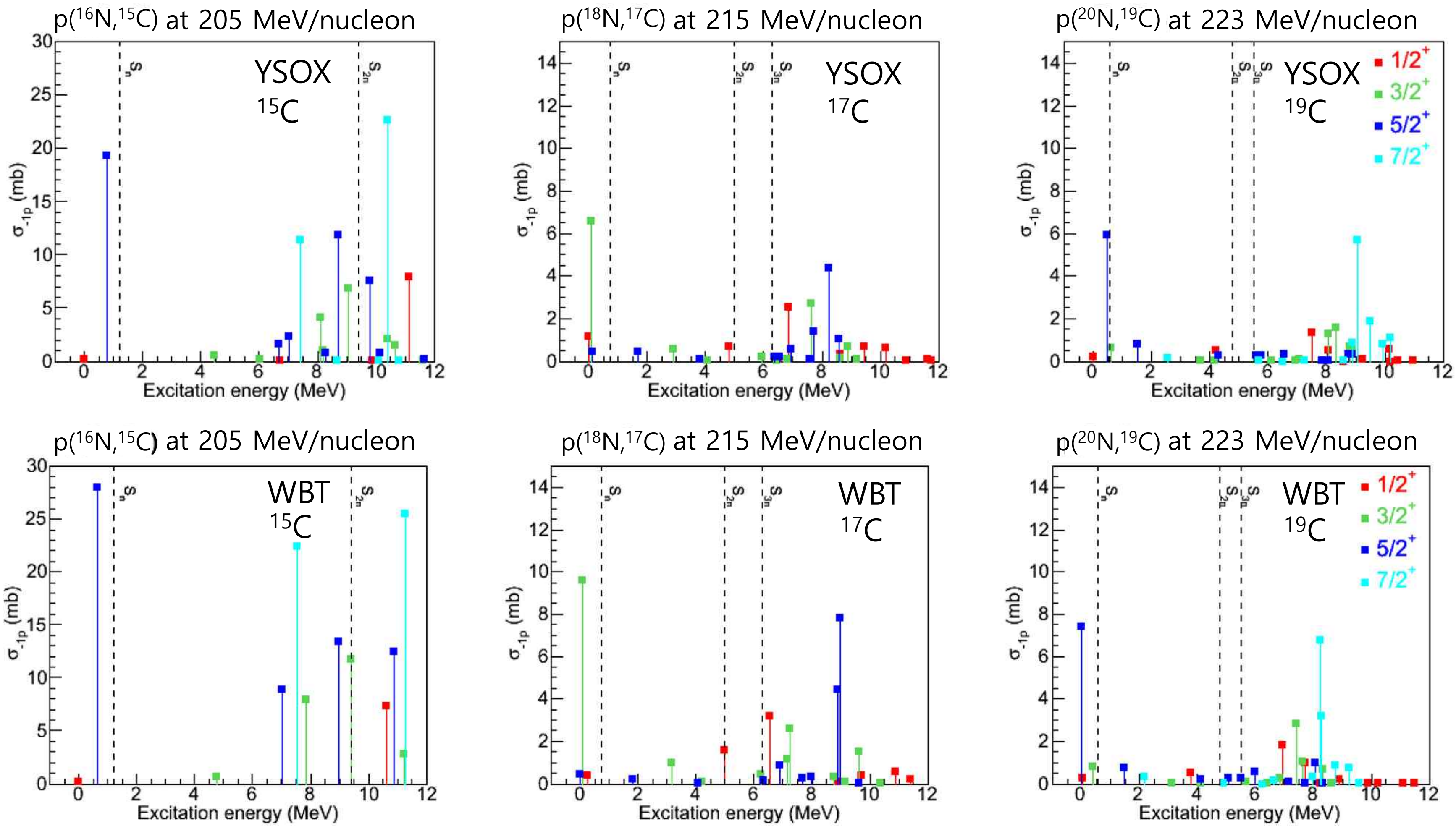

YSOX: an interaction including the π+ρ tensor force for *p-sd* cross-shell interaction

(C.Yuan et al., PRC 85, 064324 (2012))

using NuShellX (NuShell) in YSOX (WBT) for C^2S and MOMDIS for σ_{sp}

Research idea for KoBRA

Isoscalar strength of the low-energy dipole excitation (IS-LED)

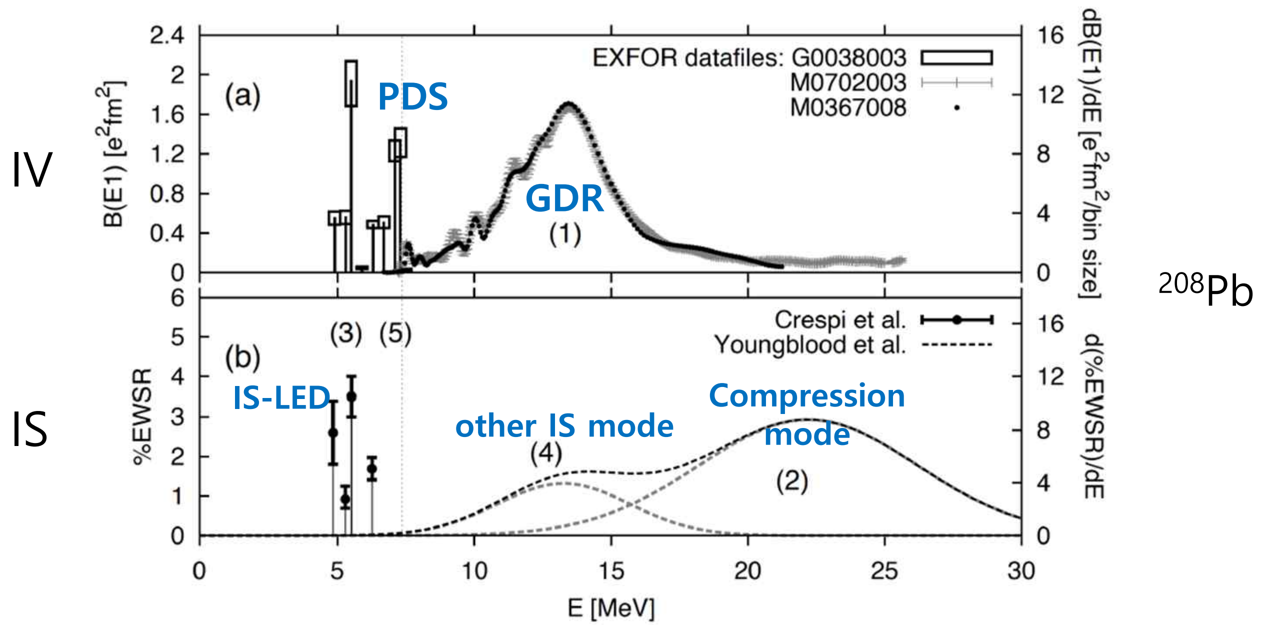

(P. Papakonstantinou, EXON-2016 (2017))

The LED strengths may indicate **emergence of possible new excitation modes** different from the GDR modes, but their properties and origins have not been clarified yet.

(Y. Shikata et al., PTEP 063D01 (2019))

Suggested dipole excitation modes to describe the LED strengths

(1) In neutron-rich nuclei, the so-called “pygmy mode” has been considered which is characterized by weakly bound valence neutron motion in the neutron skin or neutron-halo structure against a core.
(2) Another candidate is the “toroidal mode,” which is also known as the “torus mode” or “vortical mode”.
(3) Anisotropic dipole compressional mode can be another candidate for the LED excitations.

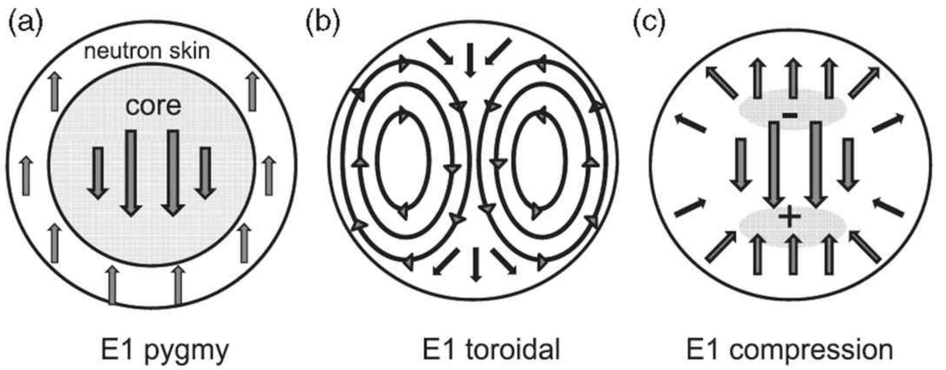

FIG. 1. Schematic velocity fields for the $E1$ pygmy (a), toroidal (b), and high-energy compressional (c) flows. The driving field is directed along the z axis. The arrows indicate only directions of the flows but not their strength. In (c), the compression (+) and decompression (−) regions, characterized by increased and decreased density, are marked.

(A. Repko et al., PRC 87, 024305 (2013))

Additionally, the cluster excitation mode can be another candidate, especially in light nuclei.

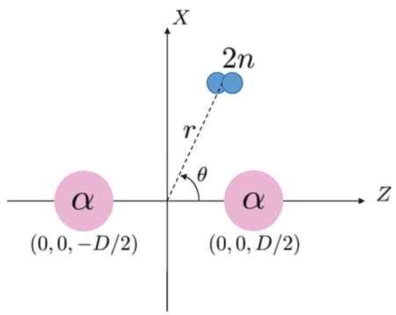

Fig. 1. Schematic figure for definitions of the parameters D, r, and θ in the $\alpha + \alpha + 2n$ model.

(Y. Shikara et al., PTEP 064D01 (2019))

Isospin character of the dipole states in N=Z and N>Z nuclei

Transition densities of the low-lying dipole states

N=Z nucleus **N>Z nucleus**

p and n transition densities

IS and IV transition densities

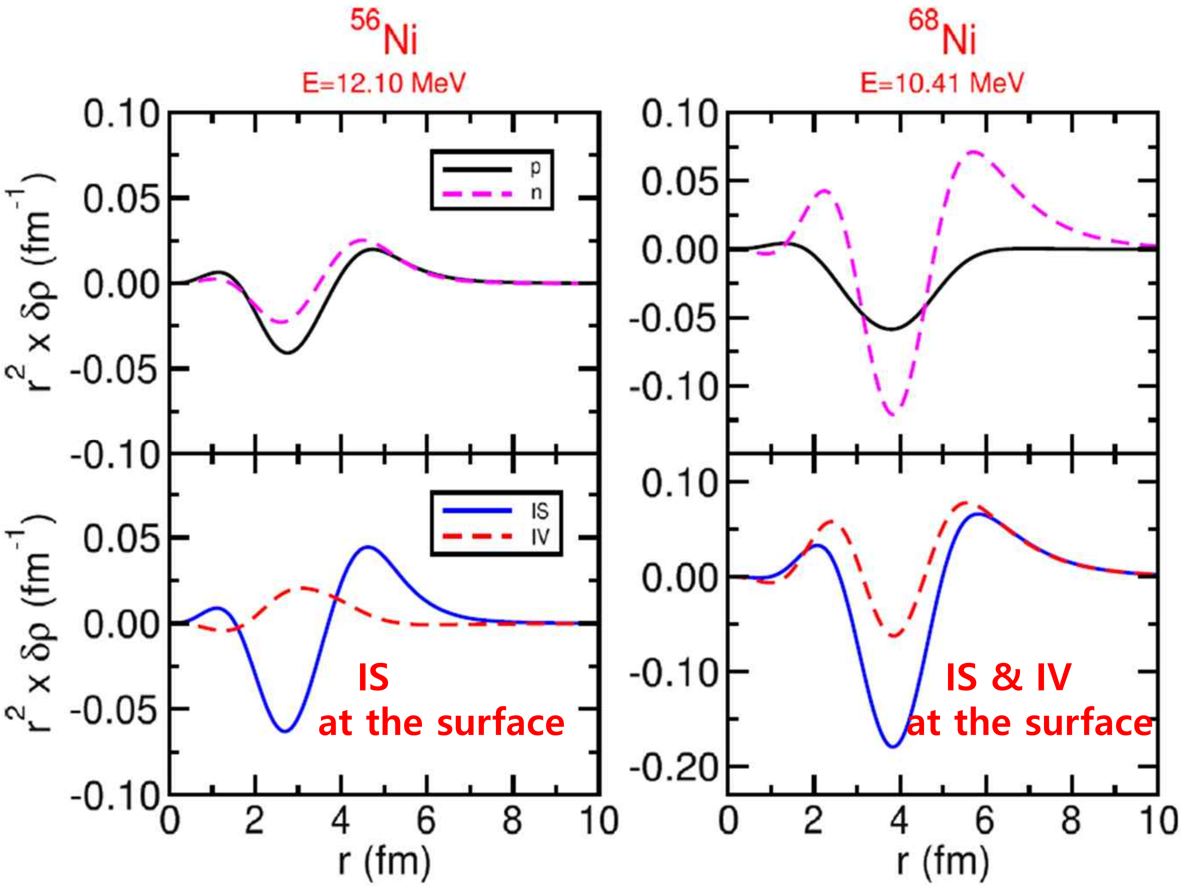

(A. Bracco et al, PPNP 106 360, (2019))

IS and IV probes and units

Dominant interaction character	Probe	Interaction	Interaction location	Units
IS	α, ^{17}O beam, (p), (^{12}C target)	Hadronic	Surface	$B_{IS}(E1)\uparrow$, IS dipole EWSR fraction, excitation cross section
IV	Photon	EM (real photon, virtual photon)	Whole nucleus	$B(E1)\uparrow$, IV dipole EWSR fraction

(Y. Shikata et al., PTEP 064D01 (2019))

For the unit of the IS dipole strength, the unit of $B_{IS}(E1)\uparrow$ has model dependence due to the nuclear radial function, so the IS dipole energy-weighted sum-rule fraction (EWSR) is often used.

$$\sigma(\alpha; 0^+_{\rm g.s.} \to 1^-) \xrightarrow{\rm DWBA} B_{\rm IS}(E1; 0^+_{\rm g.s.} \to 1^-) \to {\rm ISD\ EWSR\ (\%)}.$$

The standard unit of the IV dipole strength is $B(E1)\uparrow$.

$$\sigma({\rm Au}; 0^+_{\rm g.s.} \to 1^-) \xrightarrow{\rm DWBA} B(E1; 0^+_{\rm g.s.} \to 1^-) = B(E1)\uparrow\ (e^2{\rm fm}^2).$$

(N. Nakarsuka dissertation (2017))

IS and IV probes and units

Dominant interaction character	Probe	Interaction	Interaction location	Units
IS	α, ^{17}O beam, (p), (^{12}C target)	Hadronic	Surface	$B_{IS}(E1)\uparrow$, IS dipole EWSR fraction, excitation cross section
IV	Photon	EM (real photon, virtual photon)	Whole nucleus	$B(E1)\uparrow$, IV dipole EWSR fraction

(Y. Shikata et al., PTEP 064D01 (2019))

To study stable nuclei (target)

Possible beams: α, ^{17}O, (^{12}C, ^{13}C could be also possible as a beam)

To study unstable nuclei (beam)

Possible targets: ^{12}C, α, ^{13}C(suggested in PRL (2014))

For future experiments to investigate the IS-LED

(1) N = Z(≤20) nuclei as PP suggested (^{16}O, ^{20}Ne, ^{24}Mg, ^{28}Si, ^{32}S, ^{36}Ar, ^{40}Ca)

- **Existing data** (PRC 97, 014601 (2018), RCNP experiment)

"Systematic analysis of inelastic α scattering off self-conjugate A = 4n nuclei"
Reaction: ^{12}C, ^{16}O, ^{20}Ne, ^{24}Mg, ^{28}Si, ^{40}Ca(α,α')
Observables: excitation energies for (α,α')
$d\sigma/d\Omega$ vs $\theta_{c.m.}$ for ΔL=1

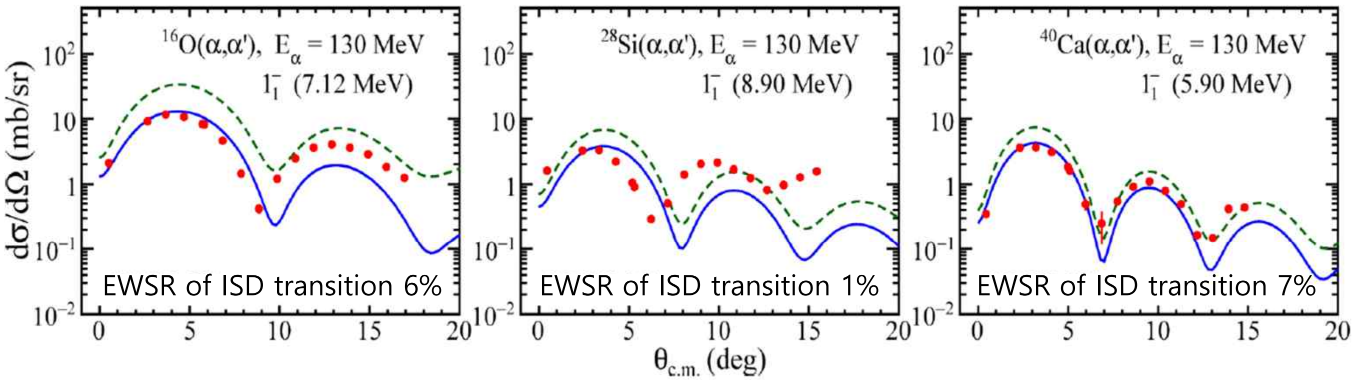

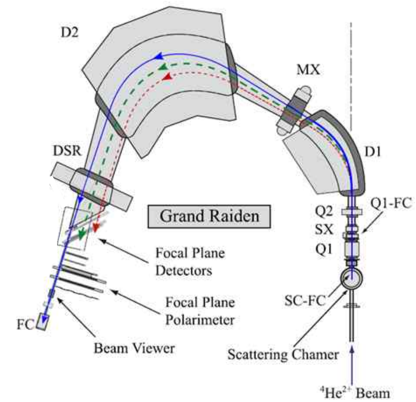

FIG. 13. Same as Fig. 6, but the cross sections for the $\Delta L = 1$ transitions at $E_\alpha = 130$ MeV. Note that the calculated cross sections are normalized to exhaust 6%, 1%, and 7% of the EWSR strengths of the isoscalar dipole transitions in ^{16}O, ^{28}Si, and ^{40}Ca, respectively.

- **What we can do**

N = Z nuclei as above including γ–ray measurement

^{32}S (recent paper: NPA(1980) elastic (α,α), quadrupole moments)
^{36}Ar (recent paper: PRC(1992) inela. 2+, 3-, 4+ → deformation parameter)

For future experiments to investigate the IS-LED

(2) Ca isotope, ^{44}Ca (or ^{40,44,48}Ca including confirmation)

- **Existing data** (PLB 730, 288 (2014), KVI experiment)

"Isospin properties of electric dipole excitations in ^{48}Ca"
Reaction: ^{48}Ca(α,α'γ) (comparison with ^{40}Ca(α,α'γ), ^{40,48}Ca(γ,γ'))
Observables: $d^2\sigma/d\Omega_\alpha d\Omega_\gamma$ vs θγ to judge dipole, quadrupole, octupole …
$d\sigma/d\Omega_\alpha$ (summed γ-ray spectrum) to get EWSR using the code

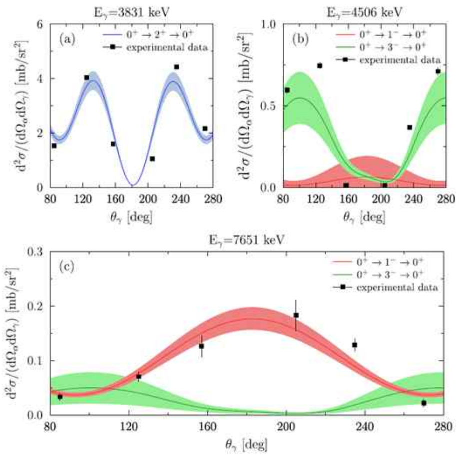

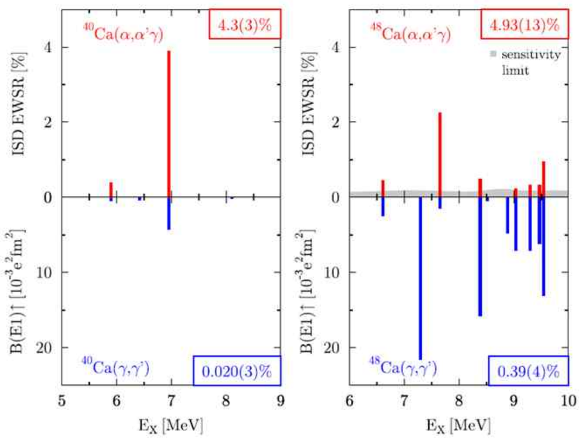

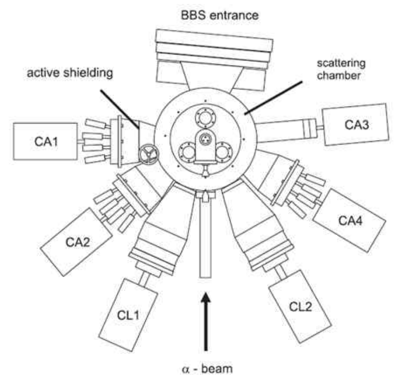

(NIMA 564, 267 (2006))

- **What we can do**

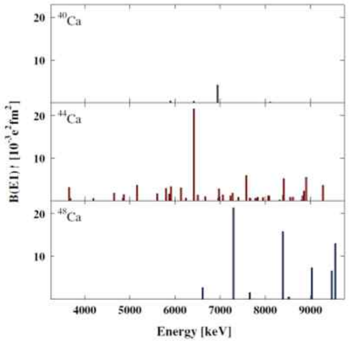

(PRC 83, 034304 (2011))

^{40,44,48}Ca(γ,γ')^{40,44,48}Ca data exist.
We can try **^{44}Ca(α,α'γ)** experiment.

Thank you
for your attention !

BACKUP

One-neutron knockout reaction

· **One-neutron knockout reaction for ^{17}C above Sn**

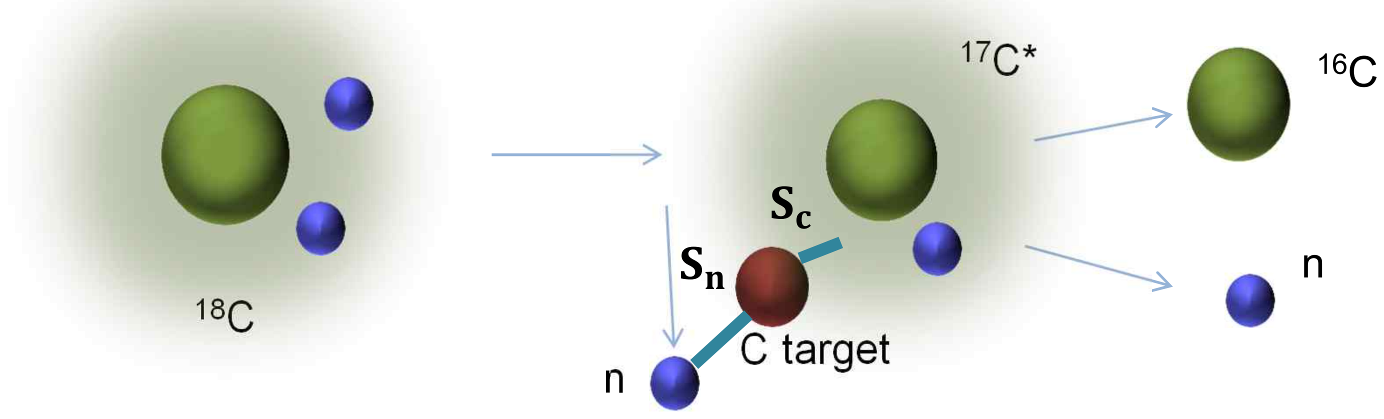

- The nucleon knockout reaction has high sensitivity to **producing the states with a hole in an orbit beneath the valence shell** with a fast moving beam.

- **Using the reaction theory based on eikonal method**, **the orbital angular momentum** can be determined by comparison of momentum spreads of the residue in the measurement and struck nucleon in the calculation.

; Parallel momentum distribution

C. A. Bertulani and A. Gade, CPC 175, 372 (2006)

$$\frac{d\sigma}{dk_z} = \frac{1}{(2\pi)^2}\frac{1}{2L+1}\sum_m \int_0^\infty d^2b_n\,[1-|S_n(b_n)\,|^2]\int_0^\infty d^2\rho |S_c(b_c)\,|^2 \left|\int_{-\infty}^\infty dz\,\exp(-ik_z Z)\,\psi_{Lm}(\boldsymbol{r})\right|^2$$

; Transverse momentum distribution

$$\frac{d\sigma}{d^2k_\perp} = \frac{1}{2\pi}\frac{1}{2L+1}\int_0^\infty d^2b_n\,[1-|S_n(b_n)\,|^2]\sum_{m,p}\int_{-\infty}^\infty dz\,\left|\int d^2\rho\,\exp(-i\boldsymbol{k}_c^\perp\cdot\boldsymbol{\rho})S_c(b_c)\psi_{Lm}(\boldsymbol{r})\right|^2$$

Branching ratio and E_{decay}

By assuming a square well potential with the centrifugal potential,

Single-particle width: $$\Gamma_{s.p.} \approx \begin{cases} \frac{2\hbar^2}{\mu R^2} \cdot kR \cdot v_l(kR) \cdot \frac{(2l-1)}{(2l+1)} & (l > 0, kR < l^{1/2}) \\ \frac{2\hbar^2}{\mu R^2} \cdot kR \cdot v_0(kR) & (l = 0) \end{cases}$$

R: radius of the daughter nucleus
k : wave number
μ : reduced mass of the decay products
v_l : transmission of a neutron through the centrifugal barrier

Partial width: $$\Gamma_i = C^2 S \cdot \Gamma_{s.p.}$$

with spectroscopic overlap C^2S between the initial and daughter state from the shell model in YSOX interaction

Branching ratio: $$\mathrm{B.R.}^{\mathrm{th}} = \Gamma_i / \sum_i \Gamma_i$$

with the width $\sum_i \Gamma_i$ for one-neutron emission

For the J^π assignment of the resonances having the $^{16}C(2^+)$ coincidence, **the branching ratios and E_{decay}** predicted by the analytic formulas and shell model calculation were taken into account.

(A.Bohr and B.R.Mottelson, Nuclear Structure I, World Scientific, 1998)